Virial coefficients for hard discs and hard spheres

1993 J. Phys. A: Math. Gen. 26 4805

(http://iopscience.iop.org/0305-4470/26/19/014)

J. Phys. A: Math. Gen. 26 (1993) 4805–4818. Printed in the UK

Virial coefficients for hard discs and hard spheres

E J Janse van Rensburg†

Department of Mathematics and Statistics, York University, 4700 Keele Street, North York, Ontario M3J 1P3, Canada

Received 13 January 1993, in final form 25 May 1993

Abstract. The sixth, seventh and eighth virial coefficients of hard discs and hard spheres are evaluated numerically (Monte Carlo integration). I improve on the best previous estimates for the seventh virial coefficients, and the integration of the eighth virial coefficient is new. The best estimates for these coefficients for hard discs are $B_7/b^6 = 0.114\,86(7)$ and $B_8/b^7 = 0.065\,14(8)$; and for hard spheres $B_7/b^6 = 0.013\,07(7)$ and $B_8/b^7 = 0.004\,32(10)$. b is the second virial coefficient in each case. Padé approximations to the excess pressure and the excess free energy are computed from these results and compared to data otherwise obtained.

1. Introduction

The thermodynamic properties of an inert fluid has long been the subject of intense investigation. Idealized models of inert fluids include hard discs (in two dimensions) and hard spheres (in three dimensions). The virial expansion of the equation of state has long been known to provide an accurate theoretical description in the fluid range (Mayer and Mayer 1940). In general, the virial expansion is an expansion of the pressure p in terms of the (number) density ρ of the fluid:

$$\frac{p}{kT} = \rho(1 + B_2\rho + B_3\rho^2 + B_4\rho^3 + \cdots) \tag{1.1}$$

where k is Boltzmann's constant and T is the temperature. The virial coefficients B_i are sums of integrals over the coordinates of i particles. Each integral is usually represented as a graph; if one follows Ree and Hoover's modification of the original Ursell–Mayer formalism (Ree and Hoover 1964, Kilpatrick 1971, Hill 1987), then

$$B_i = \frac{1-i}{i!} \lim_{V\to\infty} \frac{1}{V} \int \mathrm{d}r_1\, \mathrm{d}r_2 \ldots \mathrm{d}r_i V_i \tag{1.2}$$

where

$$V_i = \sum_{G_i} \prod_{\substack{k>l \\ k,l\in G_i}} (I(k,l)(f_{k,l} - 1) + 1)\,. \tag{1.3}$$

The virial coefficient in (1.2) is the infinite volume limit over a sum of connected, weighted clusters (or graphs) of particles. The limit over the volume can be removed by fixing one of the labelled particles at the origin. In (1.3) the cluster is expressed as a sum over labelled *blocks* G_i (sometimes called *irreducible graphs*) with i vertices. (Blocks are simple graphs

† Email address: rensburg@gibbs.math.yorku.ca

0305-4470/93/194805+14$07.50

with connectivity 2.) The product is over all pairs of labels in G_i, and I is an indicator function which is 1 if kl is in the edge-set of G_i, and zero otherwise. f is the Mayer f-function defined by $f_{k,l} = \exp(-\phi(r_k, r_l/kT)) - 1$ where ϕ is the pair-potential.

Only the first few virial coefficients have been computed for realistic potentials. The number of blocks on i vertices grows rapidly with i, and it soon becomes a considerable challenge to compute the next coefficient in the series. So far, the virial coefficients for hard discs and hard spheres have been computed up to B_7 by Ree and Hoover (1964, 1967) and by Janse van Rensburg and Torrie (1992). For both hard discs and hard spheres, B_2, B_3 and B_4 are known exactly by explicit integration. B_5 (and B_6 for hard discs) was computed accurately by Kratky (1976, 1977, 1982a, b) while Janse van Rensburg and Torrie (1992) computed B_6 and B_7 to improve on the good results of Ree and Hoover (1964, 1967) using a deterministic integration scheme (Hammersley points). B_8 is computed in this paper. (The experience with Hammersley points indicated that they perform at best only marginally better than random points in a Monte Carlo integration, if at all. Consequently, we integrated B_8 by Monte Carlo integration.) The results are tabulated in table 1. Observe that virial coefficients B_i are usually expressed as B_i/B_2^{i-1}. (The second virial coefficients B_2 are given by one half the volume of the sphere with unit radius in d dimensions, the corresponding hard sphere having unit diameter. The third virial coefficients for discs were calculated by Tonks (1936), and for spheres by Boltzmann (1899) and Happel (1906). The fourth virial coefficient for discs were calculated by Rowlinson (1963) and Hemmer (1965), and for spheres by van Laar (1899) and by Nijboer and Van Hove (1952). The best values for the fifth virial coefficients are due to Kratky (1982a,b). Kratky (1982b) also computed the very accurate value for the sixth virial coefficient of discs. The best values for the sixth virial coefficient for hard spheres, and the seventh and eighth virial coefficients for hard discs and hard spheres are those in this paper. These results are all listed in table 1.)

Table 1. Virial coefficients.

	Two dimensions	Three dimensions
B_3/B_2^2	$\frac{4}{3} - \frac{\sqrt{3}}{\pi}$	$\frac{5}{8}$
B_4/B_2^3	0.532 231 8	0.286 9495
B_5/B_2^4	0.333 556 04(4)	0.110 252(1)
B_6/B_2^5	0.198 83(1)	0.038 808(55)
B_7/B_2^6	0.114 859 (70)	0.013 071(70)
B_8/B_2^7	0.065 140 (80)	0.004 32(10)

It is possible to construct a rational (Padé) approximation to the equation of state (1.1) once a few of the virial coefficients are calculated. These Padé approximations to the equation of state have proved to be very accurate over the entire fluid range in the case of hard discs and hard spheres, which are the subject of study in this paper. It is therefore sensible to improve these Padé approximations, which we do in section 3 (see for example Ree and Hoover 1964, 1967, Valleau 1991). Ree and Hoover (1967) and Hoover and Ree (1968) developed a Padé approximation for the excess pressure and the excess free energy for hard discs and hard spheres, based on the known virial coefficients. A comparison to density scaling Monte Carlo showed remarkable agreement between the Padé and the Monte Carlo results; this is a remarkable illustration of the power of Padé approximations! (See Valleau 1991.) A more accurate Padé approximation will also improve the estimation of the radius of convergence of the virial series. While a rigorous lower bound for this is

known (Lebowitz and Penrose 1964), it seems to be far below the true radius of convergence (because of the good agreement between the Padés and numerical simulations).

2. Computational Details

The Mayer f-functions take a particularly simple form in the case of hard discs and hard spheres: the pair-potential is infinite when two discs or spheres overlap, and zero otherwise. Consequently, $f_{k,l}$ is equal to -1 if the discs or spheres with labels k and l overlap, and zero otherwise. In (1.3) we note that the contributions from two isomorphic but differently labelled blocks are exactly the same. Thus, we can write (1.3) as a sum over unlabelled blocks, if we multiply the contribution to V_i, from each unlabelled block, by the number of ways we can label the block, i.e.

$$V_i = \sum_{H_i} \prod_{e \in E(H_i)} s(H_i)\big(I(e)(f_e - 1) + 1\big). \tag{2.1}$$

Here, the sum is over all (unlabelled) blocks H_i with edge-set $E(H_i)$. $s(H_i)$ is the number of ways we can label H_i and $I(e)$ is an indicator function which is 1 if the edge e is in the set $E(H_i)$, and zero otherwise.

One can now in principle compute any virial coefficient, using either (1.3) or (2.1) as definitions for V_i. In both cases the calculation would proceed by generating labelled blocks randomly. This is done by taking a set of labelled random points, obtained subject to certain constraints, and connecting any two of them which are closer than unit distance. If the graph is a block, then in the case of (1.3), it contributes to every G_i which is a subgraph of it. Since the f-functions have a minus sign, the sign of the contribution depends on the number of edges in the block. More care has to be taken in the case of (2.1): let g_i be the number of times we can label H_i (in (2.1)) so that it is a subgraph of the generated block. Then the block contributes to the integral $g_i H_i$ if H_i is a subgraph of (the now unlabelled) block. (Observe that $g_i \neq s(H_i)$ in general; the constraints imposed on the random points usually imply that we cannot generate all labelled blocks this way.)

Ree and Hoover (1964, 1967) introduced a resummation of (2.1) which makes the calculation a bit simpler, and more efficient. Define $\hat{f} = 1 + f$, and introduce $1 = \hat{f}_e - f_e$ for every edge e which has $I(e) = 0$ (that is, the edges in the complement are assigned weights $\hat{f} - f$). The product over the Mayer f-functions and the $\hat{f}$-functions can be performed to give

$$V_i = \sum_{H_i} \prod_{e \in E(H_i)} t(H_i)\big(I(e) f_e + (1 - I(e))\hat{f}_e\big) \tag{2.2}$$

where $t(H_i)$ is the symmetry factor resulting from the resummation. It is an easy exercise to check that

$$t(H_i) = \sum_{G_i} (-1)^{|E(H_i)| - |E(G_i)|} s(G_i) h(G_i, H_i) \tag{2.3}$$

where $E(X)$ is the edge-set of X, and $h(G_i, H_i)$ is the number of distinct labellings of H_i which has a canonical labelling of G_i (see later) as a subgraph. The sum is over all unlabelled blocks. This resummation of (2.1) over a sum of *Ree–Hoover complements* has two advantages. The first is that every randomly generated block contributes potentially to exactly one integral, and secondly, many of the $t(H_i)$ turn out to be identically zero. This reduces the number of blocks which we compute significantly, and should have a marked

effect on the size of the uncertainly interval when the sum in (2.2) is carried through at the end of the calculation.

It is expensive to find the connectivity of every graph generated in the Monte Carlo integration. The best approach is to list all the blocks in a hash table before the integration, using linear probing (see Knuth (1973) for details). A query to the hash table can then determine whether a given graph is a block.

2.1. Blocks

The number of unlabelled blocks on i vertices can be determined using Polya's theorem. This number grows fast with i, if $i = 6$, then it is 56, for $i = 7$, it is 468 and for $i = 8$ it is 7123. This situation is improved with the calculation of Ree–Hoover complements in the resummation of (2.2); many of the t_i are zero. This leaves us with 23 blocks if $i = 6$, 171 if $i = 7$ and 2606 if $i = 8$. It is not an easy task to determine the number of blocks on i vertices; and it is even more difficult to find them all. There are two ways one can follow to find all blocks: the first is a building-up strategy, the second a top-down approach.

The building-up strategy works by generating new blocks on i vertices by adding a vertex to graphs on $i-1$ vertices. This appears to be an expensive operation, since one can add a vertex in 2^{i-1} ways to any given graph with $i-1$ vertices. I followed the top-down approach: Generate all graphs on i vertices and sieve out the blocks.

One can represent any labelled graph on i vertices as a string of binary digits by ordering the edges of the graph in a canonical fashion (i.e. by ordering the edges as $12, 13, \ldots, 1i, 23, 24, \ldots, 2i, 34, \ldots, (i-1)i$). If an edge is present in the graph, then the digit 1 is put in its place in the string; if it not, then the digit 0 is put in its place in the string. In this manner, every labelled graph corresponds uniquely to an integer. Unlabelled graphs are represented by the smallest integer which corresponds to a labelling of the graph. I shall think of this representation as canonical for unlabelled graphs. All the labelled graphs can now be generated in the computer by starting at the complete graph on i vertices, and subtracting 1 until we reach the integer 0, which corresponds to the null graph. Every labelled graph generated must be examined to determine whether it is a block. There is a string of theorems regarding blocks, which proved to be very helpful. (Observe that a Hamiltonian graph is always a block.) They are:

(1) If a graph has a vertex of degree 1, then it is not a block.
(2) If G is a simple graph with i vertices $x_1, x_2, \ldots, x_i$ such that $\deg(x_1) \leqslant \deg(x_2) \leqslant \ldots \leqslant \deg(x_i)$, and if $\deg(x_k) \geqslant k+1$, for each $k = 1, 2, \ldots, i-1-\deg(x_{i-1})$, then G is a block. (Bondy 1969; see Berge 1985).
(3) (Dirac) If G is a simple graph with i vertices, where $i \geqslant 3$, then if $\deg(v) \geqslant i/2$ for each vertex v in G, then G is Hamiltonian (see Wilson and Watkins 1990).
(4) If a graph G is not connected, then it is not a block.
(5) (Harary) The maximum connectivity of a connected graph with m edges and i vertices is $2m/i$ (Berge 1985).

Of course, these will not find all the blocks, and finally one has to check the graphs about which uncertainty exists directly. The computer time needed was also greatly reduced by hashing the blocks as they are found, before we try to find a canonical representation. In fact, the blocks were labelled so that the degrees of the vertices are in decreasing order, something which one must do in any case to apply Bondy's theorem. After the fact one can go and find the canonical representations. Since many blocks will have the same representation when the degrees of vertices are in decreasing order, this reduces the number of canonical representations to be computed greatly. Using this strategy, about 250 hours on

a fast workstation were needed to find all blocks on eight vertices, blocks on seven vertices were found in about 30 minutes. The Ree–Hoover complements were computed from the blocks using (2.3).

2.2. Computational methods and results

The Monte Carlo integration of the integrals represented by the Ree–Hoover complements can now proceed by generating clusters of points subject to some constraints. In the calculations of Ree and Hoover (1964, 1967), the points were generated by putting the first point at the origin. The second point is put within unit distance from the first, and the third within unit distance from the second, and so on. This arrangement is illustrated in figure 1, and one can sample any (labelled) graph which has the graph in figure 1 as a spanning subgraph. The calculation is made more efficient if there exists a number of labellings of the graph which has the graph in figure 1 as a spanning subgraph. For example, the graph in figure 2(*a*) can be labelled to have figure 1 as a spanning subgraph in two different ways. (Here, the number of vertices is 6). There are also some graphs which cannot be labelled to have the graph in figure 1 as a subgraph, and we cannot compute the contribution of the integral by sampling graphs subject to the constraint in figure 1. If the number of vertices is 6, then figure 2(*b*) is such a graph. We must therefore also generate graphs subject to a different set of constraints so that we are sure that every contribution to the virial coefficient is calculated. In the case of the sixth virial coefficient, the constraints in figure 3 were found to be enough to ensure that every integral is estimated. The number of random graphs generated for each constraint was 2.5×10^8, so that B_6 was estimated over sample size of 5×10^8 random graphs. The data were analysed in the usual way, and the result is given in table 1. The error bar is a single standard deviation. B_7 were computed by generating random graphs subject to the constraints in figure 4. Again, 2.5×10^8 random graphs were generated for each constraint, so that it was computed over a sample size of 7.5×10^8. B_8 was computed over the constraints in figure 5, again with a sample size of 2.5×10^8 for each constraint for a total sample size of 1.5×10^9. These results are in table 1.

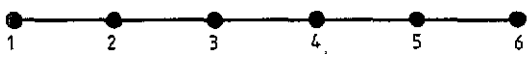

Figure 1. Random clusters of discs or spheres can be generated by putting the first sphere at the origin, the second is put within unit distance from the first, the third within unit distance from the second, and so on. In this graph, each labelled vertex corresponds to a disc or a sphere. Any labelled graph which has this graph as a spanning subgraph can be sampled by these.

Ree and Hoover (1967) extrapolated their Padé approximants to predict values for B_8/B_2^7 for hard discs and spheres. For hard discs the predicted values were 0.0635 from a $P(3, 4)$ Padé and 0.0630 from a $P(4, 3)$ Padé. Both these values are close to what was finally obtained in this paper. For hard spheres the corresponding predictions were 0.0058 from $P(3, 4)$ and 0.0049 from $P(4, 3)$, again quite close, but one can argue that the overestimation is significant. Kratky (1977) used several methods to extrapolate to higher virial coefficients for spheres. His estimates for the eighth coefficient varied between 0.0042 and 0.0052 which overlaps the calculation in this paper.

The results obtained in table 1 compare favourably with earlier estimations of the virial coefficients (the fifth virial coefficients in table 1 are due to Kratky (1977, 1982a)). B_6/B_2^5 for discs and spheres were estimated to be 0.1992(8) and 0.0386(4) by Ree and Hoover (1964, 1967) and 0.198 82(7) and 0.039 19(7) by Janse van Rensburg and Torrie (1992).

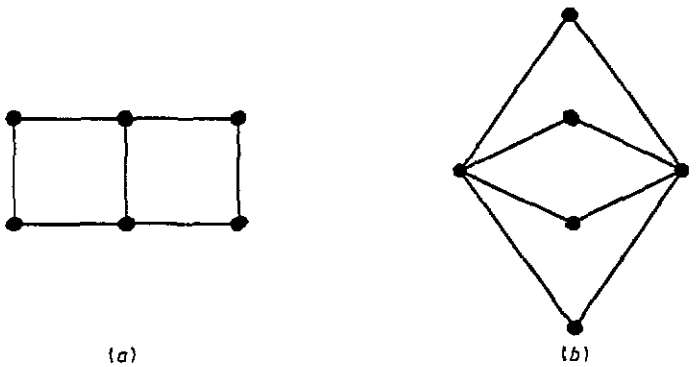

Figure 2. (*a*) This graph has two distinct labellings which has the graph in figure 1 as a spanning subgraph. (*b*) This graph has no labelling which has the graph in figure 1 as a spanning subgraph, and can consequently not be computed by generating random graphs subject to the constraints in figure 1.

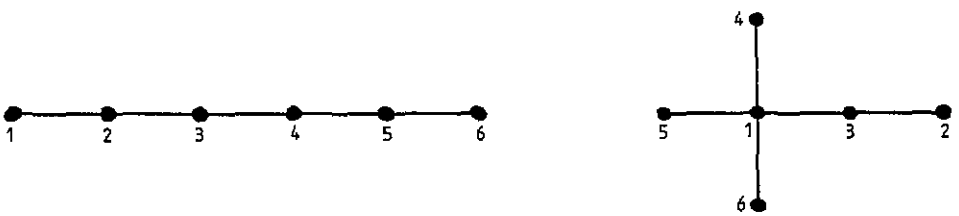

Figure 3. The random clusters used to compute the sixth virial coefficient. Every block on six vertices can be labelled to have either, or both, of these as spanning subgraphs.

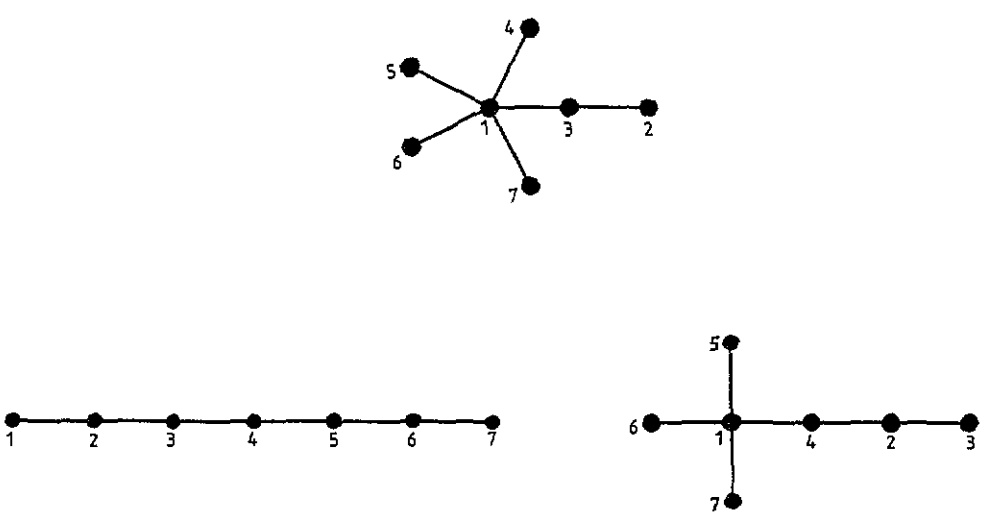

Figure 4. The random clusters used to compute the seventh virial coefficient.

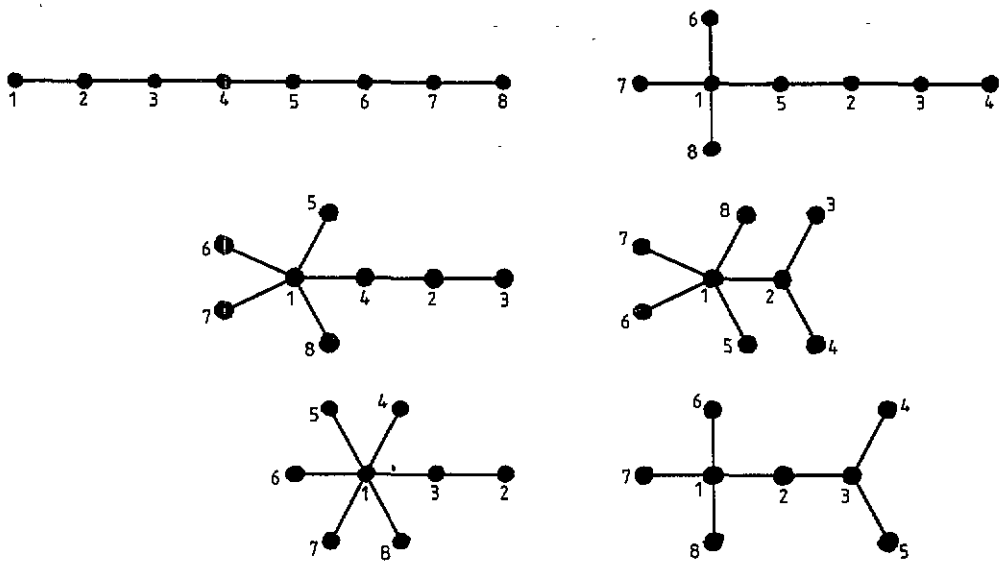

Figure 5. The random clusters used to compute the eighth virial coefficient.

The best value for discs (0.198 83(1)) is due to Kratky (1982b); for spheres, the best result is that in this paper (0.038 808(55)). For B_7/B_2^6 Ree and Hoover (1964, 1967) obtained 0.1141(5) and 0.0138(6), while Janse van Rensburg and Torrie (1992) obtained 0.114 90(9) and 0.013 11(8). All these results are in close agreement with the values computed in table 1, while the error bars in table 1 are marginally better. (The results in Janse van Rensburg and Torrie (1992) were obtained using Hammersley points in a deterministic integration scheme. This scheme turned out to be slightly better than Monte Carlo integration under the circumstances; for that reason the confidence intervals on B_6/B_2^5 and B_7/B_2^6 are not much better in this paper, despite the fact that larger samplings were done. The best values for the seventh and eighth virial coefficients are the results from the calculation in this paper.)

3. Padé extrapolations

3.1. Excess pressure

We are now in a position to add some Padé approximations for the excess pressure to the list computed by Ree and Hoover (1967). These are, for discs,

$$P_2(3,3) = \frac{b\rho - 0.200\,49(b\rho)^2 + 0.006\,07(b\rho)^3}{1 - 0.982\,50b\rho + 0.242\,16(b\rho)^2} \tag{3.1}$$

$$P_2(5,3) = \frac{b\rho - 0.126\,63(b\rho)^2 + 0.018\,96(b\rho)^3 + 0.004\,22(b\rho)^4 + 0.000\,76(b\rho)^5}{1 - 0.908\,63b\rho + 0.197\,28(b\rho)^2} \tag{3.2}$$

$$P_2(4,4) = \frac{b\rho - 0.777\,55(b\rho)^2 + 0.131\,55(b\rho)^3 - 0.002\,51(b\rho)^4}{1 - 1.559\,55b\rho + 0.818\,90(b\rho)^2 - 0.146\,40(b\rho)^3} \tag{3.3}$$

$$P_2(3,5) = \frac{b\rho - 0.725\,97(b\rho)^2 + 0.112\,78(b\rho)^3}{1 - 1.507\,98b\rho + 0.759\,79(b\rho)^2 - 0.125\,12(b\rho)^3 - 0.002\,39(b\rho)^4} \tag{3.4}$$

and for spheres,

$$P_3(3,3) = \frac{b\rho + 0.075\,46(b\rho)^2 + 0.019\,39(b\rho)^3}{1 - 0.549\,54b\rho + 0.075\,90(b\rho)^2} \tag{3.5}$$

$$P_3(5,3) = \frac{b\rho + 0.149\,62(b\rho)^2 + 0.038\,62(b\rho)^3 + 0.004\,33(b\rho)^4 + 0.000\,40(b\rho)^5}{1 - 0.475\,38b\rho + 0.048\,79(b\rho)^2} \tag{3.6}$$

$$P_3(4,4) = \frac{b\rho - 0.118\,63(b\rho)^2 + 0.009\,94(b\rho)^3 - 0.002\,90(b\rho)^4}{1 - 0.743\,63b\rho + 0.187\,76(b\rho)^2 - 0.017\,12(b\rho)^3} \tag{3.7}$$

$$P_3(3,5) = \frac{b\rho + 0.017\,98(b\rho)^2 + 0.014\,17(b\rho)^3}{1 - 0.607\,02b\rho + 0.106\,61(b\rho)^2 - 0.002\,70(b\rho)^3 - 0.000\,79(b\rho)^4} \tag{3.8}.$$

Here, b is the second virial coefficient ($b = B_2$), and ρ is the number density. It is possible to estimate the next virial coefficients from these Padé approximations. In the case of discs we found

$$B_9/B_2^8 = \begin{cases} 0.0365 & \text{from } P_2(5,3) \\ 0.0366 & \text{from } P_2(4,4) \\ 0.0366 & \text{from } P_2(3,5) \end{cases} \tag{3.9}$$

and

$$B_{10}/B_2^9 = \begin{cases} 0.0203 & \text{from } P_2(5,3) \\ 0.0206 & \text{from } P_2(4,4) \\ 0.0206 & \text{from } P_2(3,5) \end{cases} \tag{3.10}$$

and in the case of spheres we found

$$B_9/B_2^8 = \begin{cases} 0.001\,42 & \text{from } P_3(5,3) \\ 0.001\,42 & \text{from } P_3(4,4) \\ 0.001\,42 & \text{from } P_3(3,5) \end{cases} \tag{3.11}$$

and

$$B_{10}/B_2^9 = \begin{cases} 0.000\,46 & \text{from } P_3(5,3) \\ 0.000\,47 & \text{from } P_3(4,4) \\ 0.000\,47 & \text{from } P_3(3,5)\,. \end{cases} \tag{3.12}$$

The predicted values for B_9 and B_{10} are quite insensitive to the particular Padé approximation used; this should give confidence in the stability of the Padés.

The singularities in the Padé approximations are listed in table 2. (The roots in table 2 are the values of $b\rho$ at which the denominator or the numerator has zero value.) $P_2(3,3)$ for discs has singularities the density $(1.12 \pm 0.08\mathrm{i})\rho_0$, where $\rho_0 = 2/\sqrt{3}$ is the density at closest packing (the locations of the singularities are given in units of ρ_0 since the density is often reduced in this way in the literature). $P_2(5,3)$ exhibits a singularity at $1.00\rho_0$, barely inside the range of physical packings. $P_2(4,4)$ and $P_2(3,5)$ have singularities inside at densities $0.89\rho_0$ and $0.92\rho_0$, which is well inside the range of physical packings. These

Table 2. Roots in the Padés (excess pressure).

Padé		*Roots*
$P_2(3,3)$	Numerator	0, 6.12, 26.9
	denominator	2.03 ± 0.12i
$P_2(5,3)$	Numerator	0, -5.58 ± 6.09i, 2.80 ± 3.38i
	denominator	1.81, 2.79
$P_2(4,4)$	Numerator	0, 1.84, 4.73, 45.8
	denominator	1.62, 1.98 ± 0.52i
$P_2(3,5)$	Numerator	0, 2.00, 4.44
	denominator	-58.0, 1.66, 2.00 ± 0.51i
$P_3(3,3)$	Numerator	0, -1.95 ± 6.91i
	denominator	3.62 ± 0.26i
$P_3(5,3)$	Numerator	0, -5.77 ± 5.91i, 0.36 ± 6.04i
	denominator	3.07, 6.67
$P_3(4,4)$	Numerator	0, -1.32 ± 7.43i, 6.06
	denominator	2.96, 4.00 ± 1.93i
$P_3(3,5)$	Numerator	0, -0.63 ± 8.38i
	denominator	-15.60, 3.01, 4.57 ± 2.46i

Padés do not give a description of the hard disc fluid at densities higher than this, and one suspects that the approximation will be suspect in a region close to these densities. Figure 6 is a plot of $P_2(3,3)$ and $P_2(5,3)$ against some molecular dynamics data taken from Erpenbeck and Luban (1985). The radius of convergence of $P_2(3,3)$ is determined from the roots in the denominator to be $1.121\rho_0$. As Ree and Hoover (1967) observed, there is a finite maximum in $P_2(3,3)$ on the real axis at $1.12\rho_0$, and it is tempting to believe that this indicates the appearance of a thermodynamically unstable region beyond this maximum. However, this observation does not persist in the case of the higher-order Padés. Here, we observe a singularity on the real axis, which also determines the radii of convergence. The higher-order Padés appear to contain more information than $P_2(3,3)$; the finite maximum has become a singularity on the real axis, and its location has shifted towards lower density.

In the case of spheres a clearer picture emerges. $P_3(3,3)$ has singularities at $(1.22 \pm 0.09\text{i})\rho_0$ (in this case, $\rho_0 = \sqrt{2}$). Consequently, there is a finite maximum in $P_3(3,3)$ at $1.12\rho_0$ on the real axis. This maximum is replaced by singularities on the real axis in the higher order Padés. $P_3(5,3)$ exhibites a singularity at $1.04\rho_0$, $P_3(4,4)$ has it at $1.00\rho_0$ and $P_3(3,5)$ has it at $1.02\rho_0$; all close together. Indeed, there is not much difference between the higher-order Padés; in figure 7 these are plotted, and we observe that they are virtually indistinguishable from each other. The radii of convergence for each of these are given by the location of the singularities in each case; for $P_3(3,3)$ it is $1.23\rho_0$, while for the higher-order Padés it is at $1.04\rho_0$ ($P_3(5,3)$), $1.00\rho_0$ ($P_3(4,4)$), and $1.02\rho_0$ ($P_3(3,5)$). Figure 7 indicates also that these Padés approximate the molecular dynamics data (taken from Erpenbeck and Wood (1984)) quite well. There is a slight divergence between the Padés at higher density visible in figure 7, but it is not clear (from this data) which Padé would provide a better description of the system.

3.2. Excess free energy

The excess free energy A_{ex} can be expressed as an infinite series using the virial coefficients in the following way:

$$\frac{A_{ex}}{NkT} = B_2\rho\left(\sum_{i=2}^{\infty}\frac{B_i}{(i-1)B_2^{i-1}}(B_2\rho)^{i-2}\right). \tag{3.13}$$

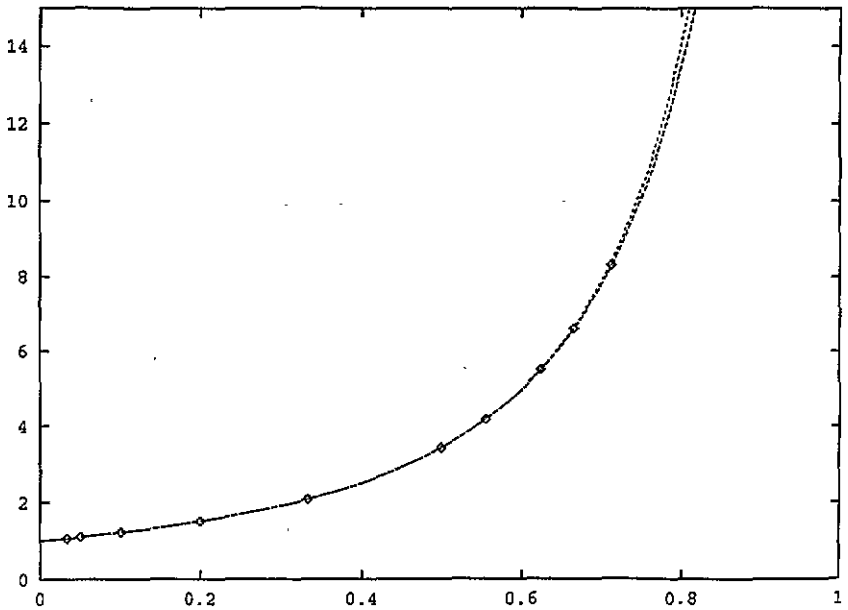

Figure 6. The reduced pressure of a fluid of hard discs against ρ/ρ_0. The data points are molecular dynamics data (Erpenbeck and Luban 1985).

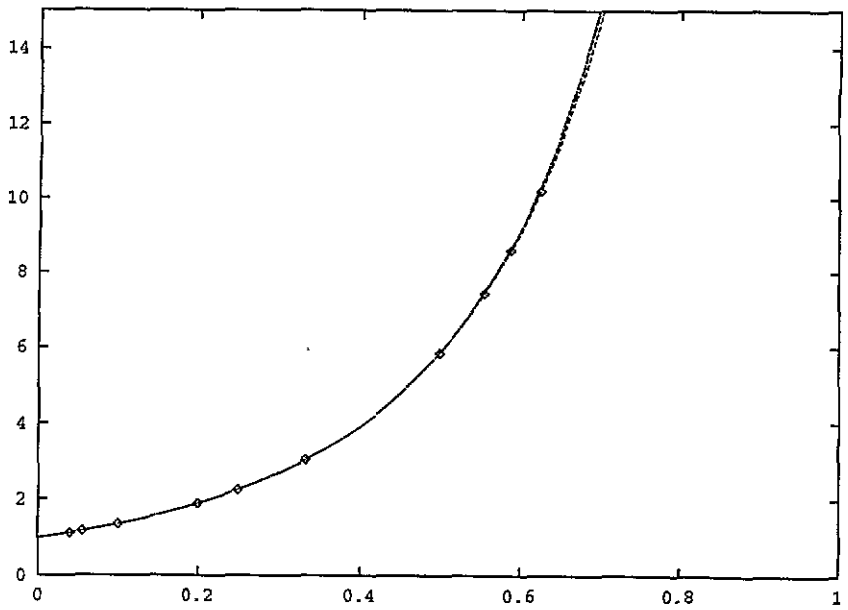

Figure 7. The reduced pressure of a fluid of hard spheres against ρ/ρ_0. The data points are molecular dynamics data (Erpenbeck and Wood 1984). All the Padé approximations describe the data well over a wide range of densities in the fluid region.

Padé approximations can now be easily computed in exactly the same fashion as for the excess pressure, except that the virial coefficients B_i are now modified by a division with $(i-1)$. For discs I obtained the following expressions (here, $Q(n,m)$ is the order-(n,m)

Padé approximant to A_{ex}/NkT):

$$Q_2(3,3) = \frac{b\rho - 0.276\,79(b\rho)^2 + 0.006\,04(b\rho)^3}{1 - 0.667\,79b\rho + 0.089\,73(b\rho)^2} \tag{3.14}$$

$$Q_2(5,3) = \frac{b\rho - 0.594\,65(b\rho)^2 + 0.032\,49(b\rho)^3 + 0.002\,55(b\rho)^4 + 0.000\,24(b\rho)^5}{1 - 0.985\,65b\rho + 0.240\,47(b\rho)^2} \tag{3.15}$$

$$Q_2(4,4) = \frac{b\rho - 0.897\,91(b\rho)^2 + 0.153\,67(b\rho)^3 - 0.002\,23(b\rho)^4}{1 - 1.288\,92b\rho + 0.480\,23(b\rho)^2 - 0.044\,71(b\rho)^3} \tag{3.16}$$

$$Q_2(3,5) = \frac{b\rho - 0.854\,80(b\rho)^2 + 0.130\,86(b\rho)^3}{1 - 1.245\,80b\rho + 0.440\,56(b\rho)^2 - 0.034\,63(b\rho)^3 - 0.005\,01(b\rho)^4} \tag{3.17}$$

and for spheres:

$$Q_3(3,3) = \frac{b\rho - 0.081\,37(b\rho)^2 + 0.004\,92(b\rho)^3}{1 - 0.393\,87b\rho + 0.032\,35(b\rho)^2} \tag{3.18}$$

$$Q_3(5,3) = \frac{b\rho + 0.809\,99(b\rho)^2 + 0.031\,99(b\rho)^3 + 0.006\,67(b\rho)^4 + 0.000\,51(b\rho)^5}{1 + 0.497\,49b\rho - 0.219\,13(b\rho)^2} \tag{3.19}$$

$$Q_3(4,4) = \frac{b\rho - 0.450\,12(b\rho)^2 + 0.042\,63(b\rho)^3 - 0.001\,77(b\rho)^4}{1 - 0.762\,62b\rho + 0.185\,30(b\rho)^2 - 0.014\,29(b\rho)^3} \tag{3.20}$$

$$Q_3(3,5) = \frac{b\rho - 0.318\,88(b\rho)^2 + 0.030\,63(b\rho)^3}{1 - 0.631\,38b\rho + 0.132\,29(b\rho)^2 - 0.008\,51(b\rho)^3 - 0.000\,35(b\rho)^4}. \tag{3.21}$$

Table 3. Roots in the Padés (excess free energy).

Padé		Roots
$Q_2(3,3)$	Numerator	0, 3.95, 41.87
	denominator	2.08, 5.365
$Q_2(5,3)$	Numerator	0, -9.87 ± 14.29i, 1.99, 7.20
	denominator	1.85, 2.25
$Q_2(4,4)$	Numerator	0, 1.48, 4.84, 62.59
	denominator	1.48, 2.09, 7.18
$Q_2(3,5)$	Numerator	0, 1.52, 5.01
	denominator	−80.58, 1.52, 2.13, 7.67
$Q_3(3,3)$	Numerator	$0, 8.27 \pm 11.61$i
	denominator	3.61, 8.57
$Q_3(5,3)$	Numerator	$0, -15.24, -1.28, 1.73 \pm 9.86$i
	denominator	−1.28, 3.55
$Q_3(4,4)$	Numerator	$0, 2.94, 10.57 \pm 8.96$i
	denominator	2.87, 4.01, 6.09
$Q_3(3,5)$	Numerator	$0, 5.21 \pm 2.36$i
	denominator	$-36.19, 3.42, 4.23 \pm 2.28$i

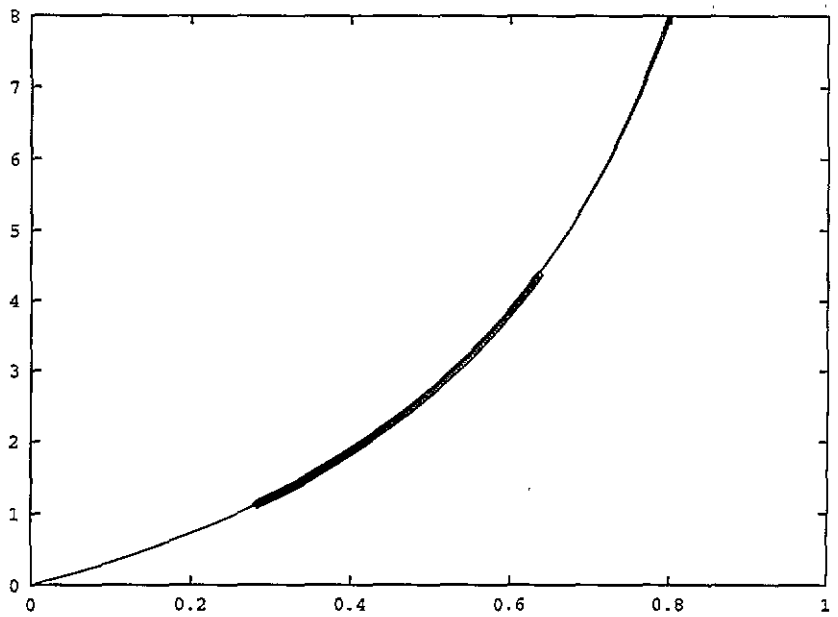

Figure 8. The reduced excess free energy of a fluid of hard spheres against ρ/ρ_0. The Padé approximations are virtually indistinguishable from each other. The data points are density scaling Monte Carlo (Valleau 1991) results.

As before, $b = B_2$. The singularities of these Padés are in table 3. For hard discs, $Q_2(3,3)$ has a singularity at $1.15\rho_0$, which also determines the radius of convergence of the approximation. This value is close to that of the Padé $P_2(3,3)$ of the excess pressure. Much of the structure of Padés computed for the excess pressure is present in the above equations in table 3 we see that singularities at low pressure in $Q_2(4,4)$ and $Q_2(3,5)$ are cancelled by roots in the numerators. If these 'unphysical' singularities are ignored, then one observes that much of the remaining structure in these approximations is close to the structure observed in $Q_2(3,3)$ above. I conclude that these Padés should be viewed with suspicion. In contrast with this, $Q_2(5,3)$ has a singularity at $1.02\rho_0$, and this also determines the radius of convergence of $Q_2(5,3)$.

In the case of hard spheres one observes a singularity in $Q_3(3,3)$ at $1.22\rho_0$, this is also the radius of convergence of this approximation. $Q_3(5,3)$ has a singularity at $-0.43\rho_0$, which is cancelled exactly (up to the numerical accuracy achieved here) by a root in the numerator. Otherwise, $Q_3(5,3)$ has a second singularity at $1.20\rho_0$, close in value to that of $Q_3(3,3)$. $Q_3(4,4)$ and $Q_3(3,5)$ have singularities at $0.97\rho_0$ and $1.15\rho_0$ respectively, which also determines the radii of convergence of these approximations. In figure 8 the Padés $Q_3(3,3)$, $Q_3(5,3)$, $Q_3(4,4)$ and $Q_3(3,5)$ are plotted. These are virtually identical, except for higher densities, where the curves start to diverge from each other. The data in figure 8 were graciously supplied by J P Valleau, obtained by a density scaling Monte Carlo simulation of 108 particles. There is no difference between those data, and the Padés computed in this section, over the entire region of reduced densities from about 0.3 to 0.65.

4. Conclusions

In this paper the eighth virial coefficient of hard discs and hard spheres were computed. This

extends the virial series in these cases to eight terms, and the description of the equation of state is becoming more accurate with the addition of each new term. The values obtained are consistent with guesses in the literature (obtained usually by extrapolating from a Padé approximation). The major difficulty in these calculations was the generation of all blocks on eight vertices. Higher virial coefficients can only be computed with great difficulty; the number of blocks on n vertices grows superexponentially, and it will soon be impossible to generate them for the next coefficient in a reasonable CPU time. There are 194 066 blocks on 9 vertices, compared to 7123 on 8 vertices, so that at best, it will take 30 times longer to generate the blocks on 9 vertices, when compared to 8.

A new graphical expansion, originally due to Lesk (1975) and generalized by Kratky (1982a) deserves closer examination. Kratky showed that the number of graphs in this expansion (the *overlap graph expansion*) is fewer than that of the Ree–Hoover expansion for the seventh virial coefficient; it is not clear whether this persists for the eighth virial coefficient, if the overlap graph expansion exists. Kratky conjectures the following: 'It is possible to express B_n for any n in terms of overlap graphs'. If this conjecture turns out to be true, then one is presented with an exciting new possible technique for evaluating virial coefficients. In addition, new work by Lieb and Sokal (1993) uses rearrangement inequalities to prove interesting bounds on virial coefficients.

A second issue which must be considered is that of important sampling techniques in the Monte Carlo simulations. Of course, the integration in this paper is in effect an important sampling, since we constrained our trial states to be from the connected graphs in figures 1 to 5. A second possible improvement would be to weight the bond-lengths between discs or spheres. However, I am unsure as to which graphs contribute the most to the virial coefficients. My data indicate that the complete graph and the cycle graph contribute much, although the first is a very compact configuration, and the second a very dilute configuration. It is thus not obvious how one should weight the bonds towards shorter (important sampling on compact configurations), or towards longer bonds (important sampling on dilute configurations).

New Padé approximations to the reduced excess free energy and to the reduced excess pressure were computed and compared to data otherwise obtained. The Padés all agree well with data obtained by molecular dynamics and Monte Carlo simulations of hard discs and hard spheres. In general, I observed little difference between the Padé approximations. Those Padé approximations with a singularity which cancels between the denominator and the numerator ($Q_2(4,4)$, $Q_2(3,5)$ and $Q_3(5,3)$) cannot be considered serious improvements compared to lower order Padés. The existence of a (mathematical) singularity (in the low density region) makes these Padés suspect, and if the cancellation is carried through, the result is a lower-order approximation. I conclude that these Padé approximations contains at best the same information as a lower-order Padé, and at worst, may be unreliable.

Lastly, the calculation of the eighth virial coefficient of other systems, such as the Lennard–Jones fluid, can be carried through without much effort. Investigators who may want to do this can obtain the list of blocks and their Ree–Hoover complements from me by email.

Acknowledgments

The author expresses his gratitude to J P Valleau and G M Torrie for numerous discussions. This work was supported by an NSERC of Canada equipment grant and an NSERC of Canada operating grant.

References

Alder B J and Wainwright T E 1962 *Phys. Rev.* **127** 359
Bondy J A 1969 *Studia Sci. Math. Hungar* **4** 473
Berge C 1985 *Graphs* (Amsterdam: North-Holland)
Boltzmann L 1899 *Verslag Gewone Vergadering Afdeling Natuurkunde Koninklike Nederlandse Akademie Wetenschap* **7** 484
Erpenbeck J J and Luban M 1985 *Phys. Rev.* A **32** 2920
Erpenbeck J J and Wood W W 1984 *J. Stat. Phys.* **35** 321
Happel H 1906 *Ann. Physik* **21** 342
Hemmer P C 1965 *J. Chem. Phys.* **42** 1116
Hill T L 1987 *Statistical Mechanics: Principles and Selected Applications* (New York: Dover)
Hoover W G and Alder B J 1967 *J. Phys.* **46** 686
Hoover W G and Ree F H 1968 *J. Chem. Phys.* **49** 3609
Janse van Rensburg E J and Torrie G M 1992 *J. Phys. A: Math. Gen.* **26** 943
Kilpatrick J E 1971 *Adv. Chem. Phys.* **20** 39
Knuth D E 1973 *The Art of Computer Programming* vol 3 (Reading, MA: Addison-Wesley)
Kratky K W 1976 *Physica* **85A** 607
—— 1977 *Physica* **87A** 584
—— 1982a *J. Stat. Phys.* **27** 533
—— 1982b *J. Stat. Phys.* **29** 129
Lebowitz J L and Penrose O 1964 *J. Math. Phys.* **5** 841
Lesk A M 1975 *J. Chem. Phys.* **63** 5048
Lieb E and Sokal A D 1993 private communication
Mayer J E and Mayer M G 1940 *Statistical Mechanics* (New York: Wiley)
Nijboer B R A and Van Hove L 1952 *Phys. Rev.* **85** 777
Ree F H and Hoover W G 1964 *J. Chem. Phys.* **40** 939
—— 1967 *J. Chem. Phys.* **46** 4181
Rowlinson J S 1963 *Mol. Phys.* **7** 593
Tonks L 1936 *Phys. Rev.* **50** 955
Valleau J P 1991 *J. Comp. Phys.* **96** 193
van Laar J J 1899 *Amsterdam Akad. Verslag* **7** 350
Wilson R J and Watkins J J 1990 *Graphs, An Introductory Approach* (New York: Wiley)